Two mode backbone curves for analysis of a rotor-stator contact system

A.D. Shaw [1], **A.R. Champneys** [2], **M.I. Friswell** [1]
[1] Swansea University, College of Engineering,
Bay Campus, Fabian Way, Swansea, SA1 8EN, UK
e-mail: **a.d.shaw@swansea.ac.uk**

[2] University of Bristol, Queen's Building,
University Walk, Bristol, BS8 1TR, UK

Abstract
Rotating machinery with a clearance between rotor and a stator can experience sustained lateral vibrations with intermittent rotor-stator contact, at frequencies removed from the linear critical speeds of the rotor or the driving speed. This motion can be highly damaging to the rotating machinery, due to the repeated impacts that occur. Previous work has shown that these types of oscillations are composed of an internal resonance between two whirling modes of the rotor, driven by out of balance forcing. The current work extends this insight, by extracting an underlying conservative model from the system and developing amplitude-frequency relations known as backbone curves. A harmonic balance approach is used, hence the model applies to relative soft stators such as a snubber rings, where contacts may have significant duration. An overhung rotor system is used to demonstrate the approach and compare it with results from time simulation.

1 Introduction

Rotor-stator contact is an issue that affects a wide variety of applications, from turbomachinery [1] to drilling for mineral extraction [2], and is driving a large body of research [3]. Many rotating devices incorporate magnetic bearing systems [4, 5], and these must be designed with consideration of the consequences of a touch-down event in response to a failure or disturbance [6]. Ehrich has compiled examples of numerous contact phenomena witnessed in tests on turbomachinery, including period-doubling bifurcation routes to chaos, subharmonic resonance and other surprising effects such as a bearing phenomenon that leads to a rotor slowly 'switching' between two amplitudes of vibration [7].

An important category of rotor stator contact is motion where the contact is repeatedly broken and restored; while many names for this motion are used in the literature (chatter, intermittent contact, rattle, bouncing) we will henceforth refer to these responses as exhibiting *partial contact*. Many works have considered these types of phenomena [7–21]. In particular, Cole and Keogh [22] emphasise the distinction between two forms of partial contact motion; *synchronous* partial that occurs at harmonics and subharmonics of the rotor shaft speed, and *asynchronous* partial contact where the frequency of impacts is apparently unrelated to the shaft speed. Asynchronous partial contact is far less understood than synchronous partial contact, largely due to the extra difficulty of identifying the fundamental response frequencies in solutions, when it is not a harmonic of the shaft speed.

A further classification may be applied to rotor-stator contact models, relating to the assumptions that are made about the impacts that occur. Many works assume *rigid* impacts; these impacts have negligible duration, and an impact model is used to relate conditions immediately before impact with those immediately

after. When this is combined with the structural dynamics of the underlying rotor, a transcendental equation emerges, which is solved to obtain the response [22, 23]. The rigid impact assumption relates these solutions to the field of piecewise-smooth dynamical systems theory [24].

This work makes the alternative assumption that the impacts are *soft*; this concerns impacts where either the rotor or stator are relatively compliant and therefore the duration of contacts is significant compared to the overall period of motion. In these cases, harmonic balance approaches are typically used. For example, Kim and Noah [25] found solutions using a harmonic balance method that assumed two fundamental frequencies, to handle the observed effect that some response frequencies were not periodic in the drive speed frequency. Von Groll and Ewins [26] performed a harmonic balance method on a system where the stator had inertia as well as stiffness, which found both constant contact solutions but also some partial contact solutions.

Further insight into asynchronous partial contact motion was given in the recent paper by Zilli *et al.* [27], which clearly demonstrated a link between the underlying linear whirl speeds of a snubbed overhung rotor and the onset of asynchronous partial contact motion. In [28], the present authors reported a generalisation of Zilli's work to apply to any two modes of a two disk system. This was shown to be a form of internal resonance, leading to to multiple steady state solutions at a single drive speed, and numerous other nonlinear phenomena including period doubling and a pathway to chaos [29].

References [27–29] give a strong insight into the dynamics of contacting rotors, but despite this their accuracy in predicting asynchronous partial contact cycles is quite limited. This is because they only make use of the underlying linear whirl speeds in predictions. The nonlinear effect of these whirl speeds increasing with amplitude is ignored, so that there are inaccuracies in the predicted onset of these cycles, and the fact that the same form of partial contact cycle is actually seen over a range of drive speeds instead of just at one cannot be modelled. By contrast, references [25, 26] can predict with high fidelity, but can be inefficient due to the need to provide the solver with a reasonable initial guess, which can be hard to find. An analysis that can explicitly chart the link between the underlying linear responses (which are well known [30]) and any possible nonlinear limit cycles is required.

The present study moves towards this through the development of backbone curves for the rotor-stator contact system. Backbone curves have been widely used as a means of understanding nonlinear structural dynamics, by tracing the frequency amplitude relationships of a conservative system [31–34]. This gives a strong insight into the resulting dynamics of the system when it is forced and damped. For the rotor-stator contact system, the backbone curve shows how internal resonance has a dramatic effect on the underlying nonlinear system leading to partial contact oscillations.

Firstly, the mathematical representation of the system is given, and the assumptions required to extract the resonant conservative parts of the system are stated. Then the method of using a modified harmonic balance to create the resulting backbone is given. The method is demonstrated on the simple case of a snubbed overhung rotor, and results are compared to simulation.

2 Derivation of backbone curves

This section firstly presents a general mathematical description of the system under consideration, and how its motion may be described in terms of whirling modes of the underlying linear conservative system. It then shows how an internal resonance between these whirling modes is a necessary condition for asynchronous periodic contact.

2.1 General description of the system

We consider a general class of multiple degree-of-freedom systems that rotate about an shaft at a constant rotating speed Ω, subject to constant out-of-balance forces. We further suppose that the free rotor has light external damping, but can be subject to frictionless contact with a single eccentric stator of fixed clearance,

at a single point on the shaft. The shaft is assumed to be torsionally and axially rigid, hence these degrees of freedom are ignored in favour of purely lateral vibration modes. The shaft is assumed to have negligible internal damping, to avoid potential instabilities [30] that are not the focus of this work. Furthermore, it is assumed that all rotor bearings are isotropic and the stator clearance is circular with the same centre as the shaft. All elements of the system behave in a manner consistent with linear assumptions apart from possible rotor-stator contact; therefore this is an example of a system with a single, local nonlinearity.

The equations of motion of this system takes the form can be written using the standard assumptions of Lagrangian mechanics as

$$\mathbf{M}\ddot{\mathbf{q}} + \Omega\mathbf{G}\dot{\mathbf{q}} + \mathbf{K}\mathbf{q} + \mathbf{C}\dot{\mathbf{q}} + \mathbf{N}(\mathbf{q}, \dot{\mathbf{q}}) = \text{Re}\left(\Omega^2 \mathbf{b_0} e^{\jmath\Omega t}\right), \tag{1}$$

where the vector $\mathbf{q} \in \mathbb{R}^n$ contains generalised rotations and displacements in a stationary coordinate frame. The matrices $\mathbf{M}$, $\mathbf{C}$ and $\mathbf{K}$ are symmetric mass, damping and stiffness matrices respectively, $\mathbf{G}$ is a skew-symmetric matrix of gyroscopic coupling terms, and the vector $\mathbf{b_0}$ captures the distribution of out of balance forces which are written in complex form [30], and $\jmath = \sqrt{-1}$. In addition, there is a nonlinear term $\mathbf{N}(\mathbf{q}, \dot{\mathbf{q}})$ representing the rotor-stator contact which we discuss later.

This system may also be considered in a coordinate frame rotating with angular speed Ω about the shaft centre line. Hence a transformation exists between the two coordinate systems:

$$\mathbf{q} = \mathbf{T}(\Omega t)\tilde{\mathbf{q}}, \tag{2}$$

where $\mathbf{T}(\Omega t)$ is a time-varying rotational transformation matrix, and $\tilde{\mathbf{q}}$ represents generalised displacements in the rotating system. Under such a transformation, Eq. (1) may be transformed to the form

$$\mathbf{M}\ddot{\tilde{\mathbf{q}}} + \Omega\tilde{\mathbf{G}}\dot{\tilde{\mathbf{q}}} + \tilde{\mathbf{K}}\tilde{\mathbf{q}} + \mathbf{C}\dot{\tilde{\mathbf{q}}} + \tilde{\mathbf{K}}_\mathbf{c}\tilde{\mathbf{q}} + \mathbf{N}(\tilde{\mathbf{q}}, \dot{\tilde{\mathbf{q}}}) = \tilde{\mathbf{b}}_\mathbf{0} \tag{3}$$

The system matrices are assumed to be isotropic, i.e. invariant under axial rotation, hence $\mathbf{M}$ and $\mathbf{C}$ remain unchanged between equations (1) and (3). However, substitution of Eq. (2) into Eq. (1) requires expansion of derivatives using the chain rule, which results in additional terms which are incorporated into the rotational forms of the gyroscopic and stiffness matrices denoted $\tilde{\mathbf{G}}$ and $\tilde{\mathbf{K}}$ respectively. The term $\tilde{\mathbf{K}}_\mathbf{c}\tilde{\mathbf{q}}$ contains forces that originate from the transformation of the term $\mathbf{C}\dot{\mathbf{q}}$ in Eq. (1), however these are kept separate from $\tilde{\mathbf{K}}\tilde{\mathbf{q}}$ for convenience when separating the conservative parts of the system from the non-conservative parts. The matrix $\tilde{\mathbf{K}}$ is symmetric, the matrices $\tilde{\mathbf{G}}$ and $\tilde{\mathbf{K}}_\mathbf{c}$ are skew symmetric. Note that all matrices with a tilde are functions of shaft speed Ω. If it is assumed that the nonlinear force acts in a purely radial direction (as in frictionless contact) and is rotationally invariant, the form of $\mathbf{N}(\mathbf{q}, \dot{\mathbf{q}})$ may be used in either coordinate system unchanged. Also note that the out of balance forcing term, has now become a constant forcing term instead of a harmonic time varying term. Specific details of these matrices and transformations are given later on.

2.2 Whirling modes of the underlying linear conservative system

If forcing, damping and nonlinearity are neglected, a linear conservative system is extracted from Eq. (3):

$$\mathbf{M}\ddot{\tilde{\mathbf{q}}} + \Omega\tilde{\mathbf{G}}\dot{\tilde{\mathbf{q}}} + \tilde{\mathbf{K}}\tilde{\mathbf{q}} = \mathbf{0} \tag{4}$$

Owing to the first derivative term in Eq. (4), it is convenient to transform it into state space form prior to solution:

$$\dot{\tilde{\mathbf{y}}} = \tilde{\mathbf{A}}\tilde{\mathbf{y}}, \quad \tilde{\mathbf{y}} = \begin{Bmatrix} \tilde{\mathbf{q}} \\ \dot{\tilde{\mathbf{q}}} \end{Bmatrix}, \quad \tilde{\mathbf{A}} = \begin{bmatrix} \mathbf{0} & \mathbf{I} \\ \mathbf{M}^{-1}\tilde{\mathbf{K}} & \Omega\mathbf{M}^{-1}\tilde{\mathbf{G}} \end{bmatrix}, \tag{5}$$

Solutions to Eq. (5) have form

$$\tilde{\mathbf{y}} = \tilde{\mathbf{w}}_i e^{\tilde{s}_i t},$$

where $\tilde{\mathbf{w}}_i$ are the first-order eigenvectors and $\tilde{s}_i$ are the eigenvalues which are purely imaginary. From the definition of $\tilde{\mathbf{y}}$, the first order eigenvectors must have form $\tilde{\mathbf{w}} = [\tilde{\mathbf{v}}_i \ , \ s_i\tilde{\mathbf{v}}_i]^T$, and therefore it is possible to extract the second order eigenvectors that satisfy Eq. (4) directly with:

$$\tilde{\mathbf{q}} = \tilde{\mathbf{v}}_i e^{\tilde{s}_i t}$$

If the number of degrees of freedom in Eq. (4) is n, there are $2n$ degrees of freedom in Eq. (5) and hence there are $2n$ eigenvalues and associated eigenvectors. The mode shapes are complex and appear in conjugate pairs, so that a motion based on a single conjugate pair of eigensolutions will have form:

$$\tilde{\mathbf{q}} = p_i\tilde{\mathbf{v}}_i e^{\tilde{s}_i t} + p_i^*\tilde{\mathbf{v}}_i^* e^{\tilde{s}_i^* t}, \tag{6}$$

where an asterisk indicates complex conjugation and p_i is a complex amplitude. Evaluating Eq. (6) at any convenient point along the shaft will show a displacement that follows a circular path around the centre line, at an angular speed $\tilde{\omega}_i$, known as the whirl speed. If the motion is anticlockwise (the same direction as shaft speed Ω) the whirl speed $\tilde{\omega}_i$ is defined as positive, and the motion is described as a forward whirl mode. Otherwise the motion is described as a backward whirl mode, and $\tilde{\omega}_i$ is negative. It may be shown that all eigenvalue pairs may be expressed as:

$$\tilde{s}_i \ , \ \tilde{s}_i^* = \pm j\tilde{\omega}_i,$$

and that all motions of the conservative system can be expressed as a superposition of multiple whirl modes in the form of Eq. (6).

A similar analysis could be performed starting with Eq. (1) instead of Eq. (3), hence deriving whirl modes in the stationary coordinate system. However, it can be seen from the form of the transformation between the two systems that whirl speeds in the stationary system will be related to those in the rotating system by:

$$\omega_i = \tilde{\omega}_i + \Omega \tag{7}$$

and that the whirl mode shapes will be identical. This relationship allows the possibility that a forward whirl mode in the stationary system is a backward whirl in the rotating system, if $\Omega > \omega_i$. In the majority of rotor dynamics literature, the greatest attention is paid to modes that represent forwards whirl in the stationary frame, as these are typically excited by the out of balance forces and therefore determine critical rotation speeds. However, in this work all modes, either backwards or forwards, are equally relevant because impacts with the stator can excite any mode.

2.3 Extraction of the underlying conservative system

The underlying conservative system is derived from Eq. (3) as

$$\mathbf{M}\ddot{\tilde{\mathbf{q}}} + \Omega\tilde{\mathbf{G}}\dot{\tilde{\mathbf{q}}} + \tilde{\mathbf{K}}\tilde{\mathbf{q}} + \mathbf{N}(\tilde{\mathbf{q}} + \tilde{\mathbf{q}}_\mathbf{0}) = \mathbf{0} \tag{8}$$

This is mostly a straightforward matter of removing forcing and damping terms, however the form of the nonlinearity has also been altered to include the addition of a time-constant synchronous displacement term $\tilde{\mathbf{q}}_\mathbf{0}$. The reason for this is that the out of balance force has been seen to be a necessary component of asynchronous partial contact motion, but this forcing creates a non-conservative system. However, without the forcing term $\tilde{\mathbf{b}}_\mathbf{0}$ there is nothing to create a constant displacement, which is an important feature because it breaks the axisymmetry of the multiple whirling modes inside the assumed circular stator. By specifying a constant term, this symmetry breaking effect is maintained whilst keeping the system conservative.

Experience with previous simulations suggests that $\tilde{\mathbf{q}}_\mathbf{0}$ is typically very similar to the linear synchronous response, even in the presence of substantial nonlinearity, when partial contact motion occurs. Therefore, if performing analysis with reference to a known system, Eq. (3) can be rearranged to estimate $\tilde{\mathbf{q}}_\mathbf{0}$ as:

$$\tilde{\mathbf{q}}_\mathbf{0} = \left(\tilde{\mathbf{K}} + \tilde{\mathbf{K}}_\mathbf{c}\right)^{-1}\tilde{\mathbf{b}}_\mathbf{0} \tag{9}$$

2.4 Transformation to complex modal coordinates

In order to view the system response as a composition of different whirl modes, Eq. (8) is transformed to

$$\bar{\mathbf{M}}\ddot{\mathbf{p}} + \Omega\bar{\tilde{\mathbf{G}}}\dot{\mathbf{p}} + \bar{\tilde{\mathbf{K}}}\mathbf{p} + \mathbf{N_p}(\mathbf{p} + \tilde{\mathbf{p}}_\mathbf{0}) = \mathbf{0} \tag{10}$$

The complex vector $\mathbf{p}$ is related to $\mathbf{q}$ by

$$\mathbf{q} = \mathbf{\Phi}\mathbf{p} \tag{11}$$

where $\mathbf{\Phi}$ is a matrix of second order eigenvectors $\tilde{\mathbf{v}}_i$, and $\bar{\bullet} = \mathbf{\Phi}^\dagger \bullet \mathbf{\Phi}$ where $\mathbf{\Phi}^\dagger$ is the adjoint matrix of $\mathbf{\Phi}$. The nonlinear part of the equation $\mathbf{N_p}(\mathbf{p} + \tilde{\mathbf{p}}_\mathbf{0})$ is found by

$$\mathbf{N_p}(\mathbf{p}) = \mathbf{\Phi}^\dagger \mathbf{N}(\mathbf{\Phi}\mathbf{p}) \tag{12}$$

and the synchronous displacement is transformed by $\tilde{\mathbf{q}}_\mathbf{0} = \mathbf{\Phi}\tilde{\mathbf{p}}_\mathbf{0}$. The number of modes to include in $\mathbf{\Phi}$ can be chosen based on the desired accuracy; however typically just 2 can be used, because we can make an assumption about the two modes that are in internal resonance and assume that these dominate.

2.5 Assumed solution form

The assumed solution form is

$$\mathbf{p} = \sum_{i \in \mathbf{S}} \mathbf{P}_i e^{i\tilde{\omega}_r \jmath t} \ , \ \mathbf{S} \subseteq \mathbb{Z} \tag{13}$$

where $\mathbf{P}_i = [P_{i,1}, P_{i,2}, \cdots]^T$ is a vector of the complex amplitudes of each modal variable at the given nonlinear response frequency $i\tilde{\omega}_r$. This is a Fourier series representation of a rotor motion that is periodic in the rotating coordinate system. Note that due to the rotating nature of the system, the frequencies are signed according to the direction of rotation, and hence $\mathbf{S}$ may include negative integers. As many values for i are used as deemed necessary for accuracy, however, since we are typically searching for an assumed internal resonance between two modes, just two can be selected with reasonable accuracy. In the case of two-to-one resonance presented here, $\mathbf{S} = \{-1, -2\}$ is used.

2.6 Solution and back bone creation process

Equation (13) is substituted into Eq. (10). This can then be solved by matching terms for each harmonic component and modal variable combination represented by $P_{i,j}$, forming a system of harmonic balance equations in the form:

$$\mathbf{\Gamma}(\tilde{\omega}_r)\mathbf{Z} + \mathbf{n}(\mathbf{Z}) = \mathbf{0} \tag{14}$$

where $\mathbf{Z}$ is a vector of all values $P_{i,j}$, $\mathbf{\Gamma}(\tilde{\omega}_r)$ arises from substituting (13) into the linear parts of Eq. (10), and $\mathbf{n}(\mathbf{Z})$ gives Fourier coefficients arising from the nonlinearity. Before we can solve for $\mathbf{Z}$ we must evaluate $\mathbf{n}(\mathbf{Z})$ and establish the fundamental nonlinear frequency $\tilde{\omega}_r$.

The first issue is met with an Alternating Frequency Time (AFT) process, and by noting that since the conservative parts of the nonlinearity has no velocity dependence, there is no dependence on $\tilde{\omega}_r$ when evaluating Fourier components. Hence, we can temporarily assume $\tilde{\omega}_r = 1$, and evaluate $\mathbf{N_p}(\mathbf{p} + \tilde{\mathbf{p}}_\mathbf{0})$ in the time domain over a period $2\pi/\tilde{\omega}_r$ split into a suitable number of time steps. The result can then be returned to the frequency domain via a discrete Fourier transform.

The fundamental frequency is established by noting that, once the nonlinear coefficients are established, each of the harmonic balance equations becomes a quadratic equation in $\tilde{\omega}_r$. This is because the double and single derivative terms in Eq. (10) gives rise to terms of $\tilde{\omega}_r^2$ and $\tilde{\omega}_r$ respectively. Therefore, we use one equation to solve $\tilde{\omega}_r$ with the quadratic formula. In general this will fail to solve all the remaining harmonic balance

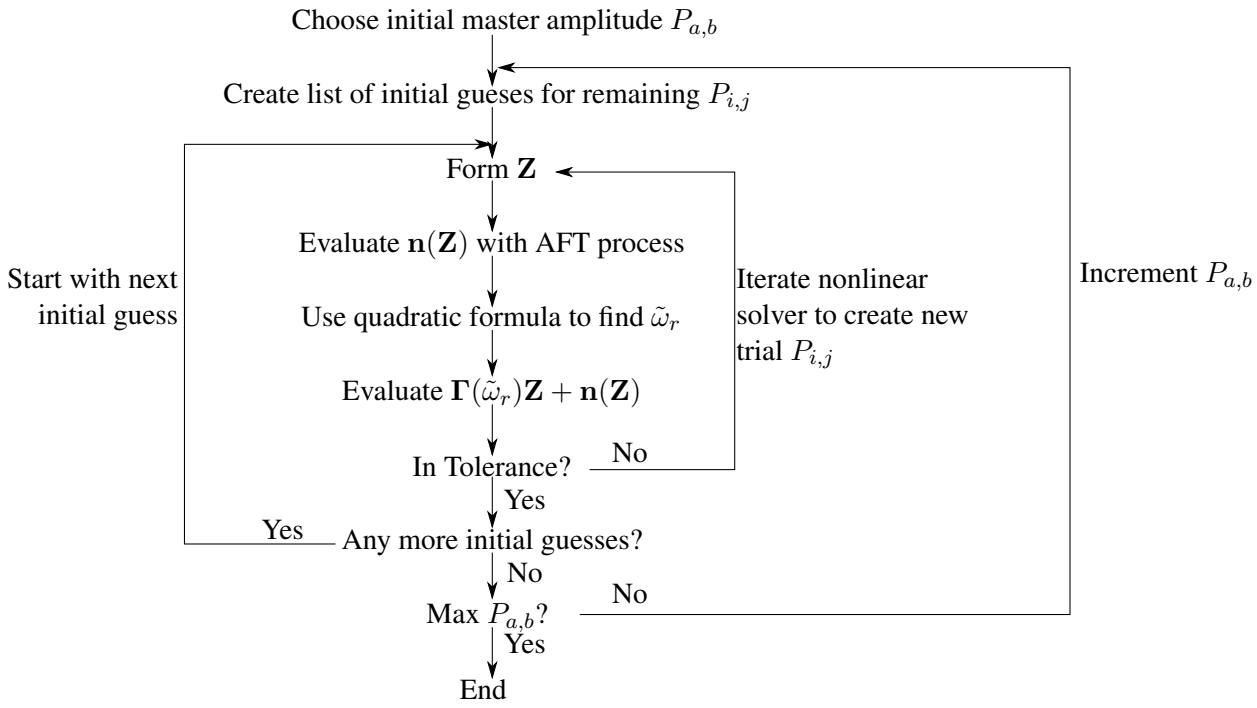

Figure 1: Flow chart of backbone creation process.

equations simultaneously; therefore this process must be iterated within a nonlinear numerical solver until a set of inputs $P_{i,j}$ is found to achieve a solution.

Typically there will be infinitely many solutions to the harmonic balance equations, so a graph is created by fixing one value $P_{i,j}$ as the master amplitude, locating all solutions by starting from a range of initial guesses, then incrementing the master amplitude and repeating to create a graph of solutions. The overall process is summarised in flow chart form in Fig. 1.

3 Simple example: a snubbed overhung rotor

We now give an a example of this model applied to a nondimensional snubbed overhung rotor. Firstly the system is described and the system matrices presented. We then present a linear analysis of where internal resonance could occur. We then go on to present backbones, highlighting the drastic qualitative changes that occur when internal resonance occurs. Finally, a brief comparison with simulations is given.

3.1 Rotor description

We now demonstrate the results of this model applied to a nondimensional model of a snubbed overhung rotor, as shown in Fig. 2, which is similar to the system studied by Zilli *et al.* [27]. This system has just two degrees of freedom and as such is the simplest form of system represented by Eq. (1).

The stationary system matrices as required by Eq. (1) are as follows:

$$\mathbf{M} = \begin{bmatrix} 1 & 0 \\ 0 & 1 \end{bmatrix} \quad , \quad \mathbf{G} = \begin{bmatrix} 0 & 0.14 \\ -0.14 & 0 \end{bmatrix} \quad , \quad \mathbf{K} = \begin{bmatrix} 1 & 0 \\ 0 & 1 \end{bmatrix} \quad , \quad \mathbf{C} = \begin{bmatrix} 0.02 & 0 \\ 0 & 0.02 \end{bmatrix} \tag{15}$$

It can be shown that the rotating system matrices as required by Eq. (3) are given by:

$$\tilde{\mathbf{G}} = \mathbf{G} + 2\mathbf{M}\mathbf{J} \tag{16}$$

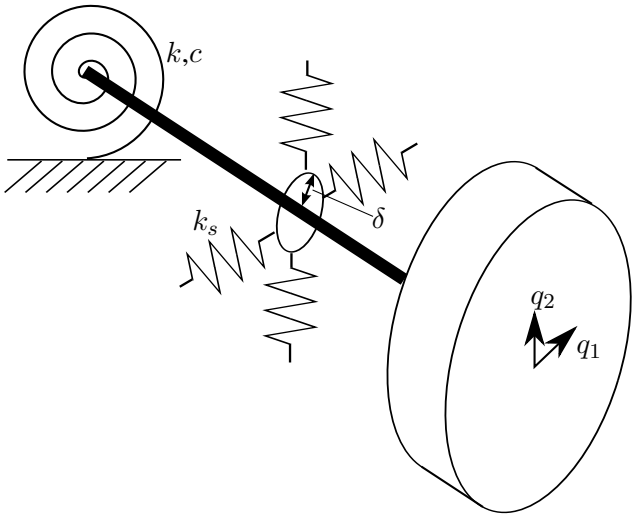

Figure 2: A snubbed overhung rotor.

$$\tilde{\mathbf{K}} = \mathbf{K} - \Omega^2\mathbf{M} + \Omega^2\mathbf{GJ} \tag{17}$$

and

$$\tilde{\mathbf{K}}_c = \Omega\mathbf{CJ} \tag{18}$$

where $\mathbf{J} = \begin{bmatrix} 0 & -1 \\ 1 & 0 \end{bmatrix}$.

The nonlinear term is given by:

$$\mathbf{N}(\mathbf{q}, \dot{\mathbf{q}}) = \begin{cases} -k_s(r-\delta) \begin{Bmatrix} q_1 \\ q_2 \end{Bmatrix} /r, & \text{if } r \geq \delta \\ \begin{Bmatrix} 0 \\ 0 \end{Bmatrix}, & \text{if } r < \delta, \end{cases} \tag{19}$$

where $r = \sqrt{q_1^2 + q_2^2}$ and the clearance is $\delta = 1$.

3.2 Linear analysis of whirl modes and potential internal resonance

The overhung rotor will have just two whirl speeds, traditionally referred to as the forward whirl speed and the backward whirl speed in the stationary coordinate system. These can be readily calculated as described in Section 2.2. In Fig. 3, the rotating coordinate system equivalents of these two speeds are presented as a function of drive speed Ω, where $\tilde{\omega}_f$ is the rotating system equivalent of the forward whirl speed and $\tilde{\omega}_b$ is the equivalent of the backward whirl speed.

Note that $\tilde{\omega}_f$ passes through zero at $\Omega \approx 1.1$; this indicates the first critical speed of the shaft. Above this speed, $\tilde{\omega}_f$ is always negative, hence the forward whirl in the stationary system is a backward whirl in the rotating system.

At $\Omega \approx 3.25$ the line of $2\tilde{\omega}_f$ crosses that of $\tilde{\omega}_b$. This implies that in the vicinity of this region is potential for a 2:1 internal resonance between the backward and forward modes. This is all that the linear analysis can tell us; however the experience of references [27–29] suggest that this an approximate indication of the onset of asynchronous partial contact limit cycles.

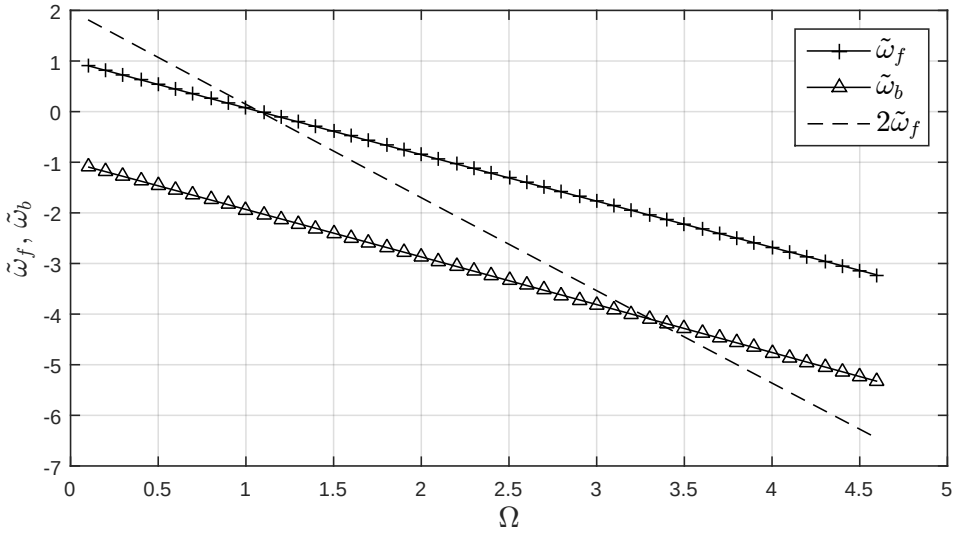

Figure 3: Campbell diagram showing whirlspeeds in the rotating system as a function of shaft speed Ω.

3.3 Backbone analysis

The modeshapes will be $\tilde{\mathbf{v}}_i = \begin{Bmatrix} 1 & \pm\jmath \end{Bmatrix}^T$, which gives simple circular orbits. However, we discard one half of the conjugate pairs of modeshapes, and just use the modeshape $\begin{Bmatrix} 1 & -\jmath \end{Bmatrix}^T$ because this has the convenient property that a motion given by $\begin{Bmatrix} 1 & -\jmath \end{Bmatrix}^T \mathrm{e}^{\jmath i\tilde{\omega}_r t}$ gives a forward whirl when $i\tilde{\omega}_r$ is positive and a backward whirl when it is negative.

Since the modeshape is the same for both the forward and backward whirls, the underlying linear system reduces to an equation in just one complex variable after the modal transformation. We are searching for a 2:1 resonance, and furthermore note that both whirl speeds are negative in the rotating frame, hence we choose $\mathbf{S} = \{-1, -2\}$ and can expand Eq. (13) as:

$$p = -P_{-1,1}\mathrm{e}^{-\jmath\tilde{\omega}_r t} - 2P_{-2,1}\mathrm{e}^{-2\jmath\tilde{\omega}_r t} \tag{20}$$

We choose $P_{-1,1}$ as the 'master' amplitude - we will fix this at different values and solve for $P_{-2,1}$. It is natural to choose positive real values for $P_{-1,1}$, and this fixes the phase of solutions. Furthermore, it emerges that for such a simple system, this leads to $P_{-2,1}$ being real as well. Therefore, in presenting results a shorthand form is used where $P_1 = P_{-1,1}$ and is always real positive, and $P_2 = P_{-2,1}$ which is real but potentially negative or positive, reflecting the phase relative to P_1. Furthermore, we assume the synchronous component is also positive and real, and given by P_0. Figure 4 gives a schematic of the simplified kinematics of motion that we have assumed.

Figure 5 shows the backbone curve analysis for a drive speed Ω that is below the value where Fig. 3 suggests internal resonance may occur. Firstly we notice a vertical region of the P_1 response; this is the linear response region and it can be seen the the response frequency $\tilde{\omega}_r$ coincides with that predicted in Fig. 3 for the drive speed concerned. However, once the amplitude is sufficient to establish contact, the frequency increases rapidly with amplitude. There is little contribution from P_2 suggesting that this is a branch of constant contact solutions (the results of references [27–29] show that there must be significant amplitude in both modal responses to give partial contact motion).

Now consider a backbone where the drive speed Ω is above the linear prediction for internal resonance; this is shown in Fig. 6. The feature that existed in Fig. 5 still exists; there is a region of non-contacting linear response (AB) leading to a region of constant contact response. However, as we move through this region,

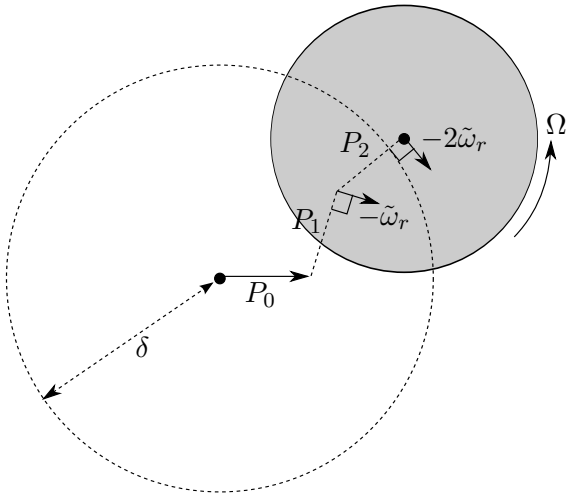

Figure 4: Schematic of the assumed kinematics of the rotor in the rotating coordinate frame.

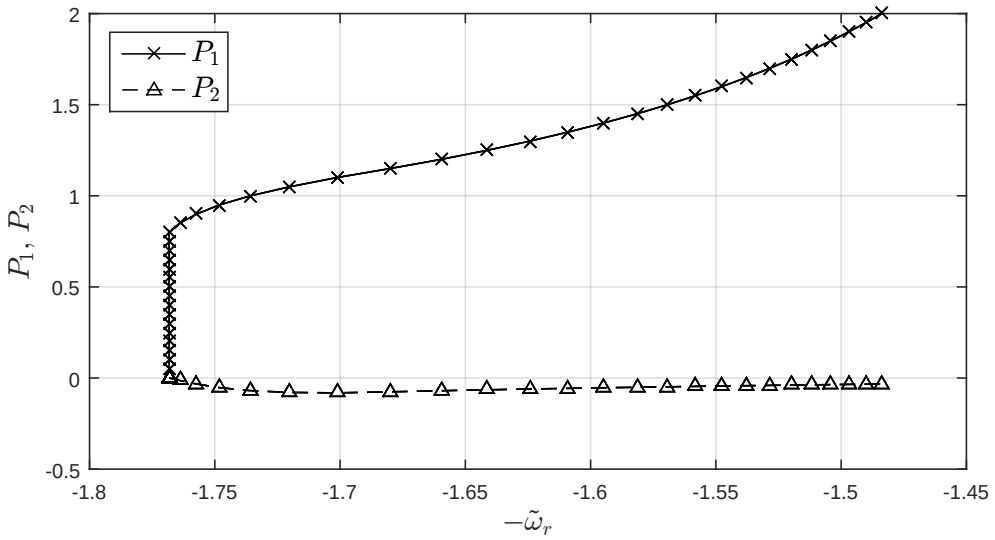

Figure 5: Backbone curves for overhung rotor at $\Omega = 3.0$, $P_0 = 0.2$.

the P_1 component begins to fall, and a significant P_2 response develops as shown in the section of P_2 with the same x-axis range as segment BC.

However, at $\Omega \approx 2.39$ we see a set of responses, where P_1 follows line DEF. Responses on segment DE are partial contact responses; the segment EF converges to a constant contact P_1 response. The fact that Figures 5 and 6 are so qualitatively different, coupled with the insight of Fig. 3, indicates that internal resonance has induced new bifurcations into our system response.

As yet, the formal stability analysis of these solutions has not been performed. However, numerical time-simulation of this system suggests that, in this region, all stable partial contact cycles reside near the range of solutions DE.

3.4 Comparison to simulation

Simulations of the complete forced and damped system were run to see how the results of backbone analysis compare. Clearly, the backbone analysis relates to the underlying conservative system, and so a direct comparison is not possible. The following procedure was used to get the best comparison possible:

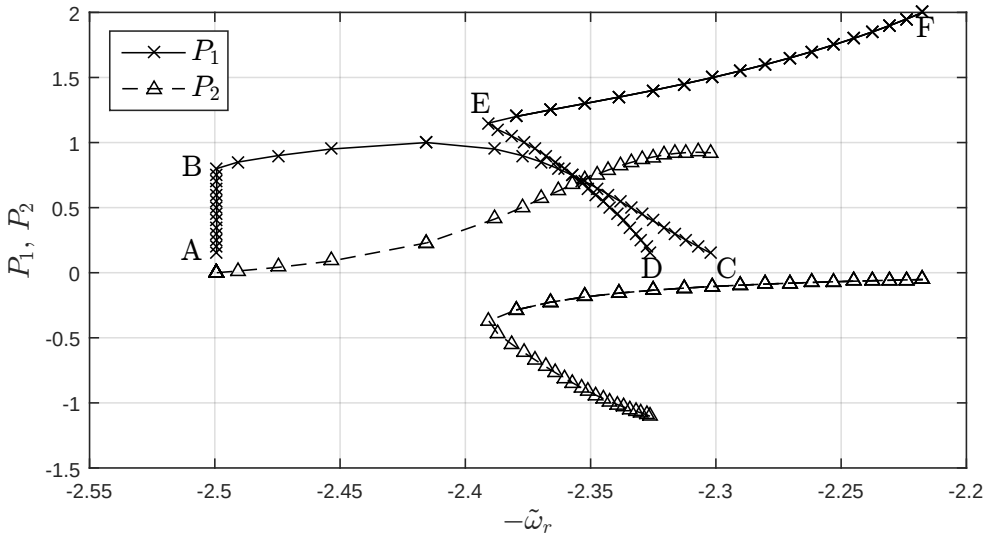

Figure 6: Backbone curves for overhung rotor at $\Omega = 3.8$, $P_0 = 0.2$.

1. The ODE45 time simulation of the overhung rotor was run at values of Ω between 3 and 4, with varying levels of out of balance and initial conditions designed to promote the partial contact limit cycle if possible.

2. If a partial contact cycle was found, the period of the motion (in the rotating coordinate system) was found by timing a complete orbit, giving the fundamental frequency $\tilde{\omega}_r$.

3. The fundamental frequency was used to calculate the relevant Fourier coefficients of the simulation. Despite being generally complex values, these were found to approximately match our assumption of being exactly in or out of phase, so the complex amplitudes are shown as $|P_1|$ and $-|P_2|$ in results.

4. In order to calculate backbone curves, the synchronous term was calculated for the relevant shaft speed using Eq. (9).

5. The amplitude P_1 was interpolated from the segment of backbone DE in Fig. 6, using $\tilde{\omega}_r$ extracted from simulation. Similarly, P_2 was interpolated from the corresponding section on the P_2 graph.

Figures 7 shows the results of this process for cases where are a partial contact orbit was found in simulation for the range of Ω shown; as can be seen the backbone results are quite similar to those from the simulated full system. However, the difference between the results seems to increase with amplitude and Ω. The reason for this can be partly explained by Fig. 8; this is an Argand plot of the full complex amplitudes found in simulation, where time has been shifted so that P_1 always lies on the positive real axis. This shows that at the lower end of the range of Ω shown, the assumption of the two amplitudes being approximately opposite in phase is reasonable; however as Ω increases the relative phase angle between the two amplitudes tends towards $135°$, hence the idealised system used for backbone analysis is less realistic.

4 Conclusions

This work has performed a backbone curve analysis of asynchronous partial contact limit cycles for a rotor stator contact system, and has the potential to greatly improve predictions concerning the onset and severity of these motions. The proposed method has been shown to give insight for a simple rotor stator contact system, and is shown to have approximate agreement with a time simulation for a forced and damped rotor.

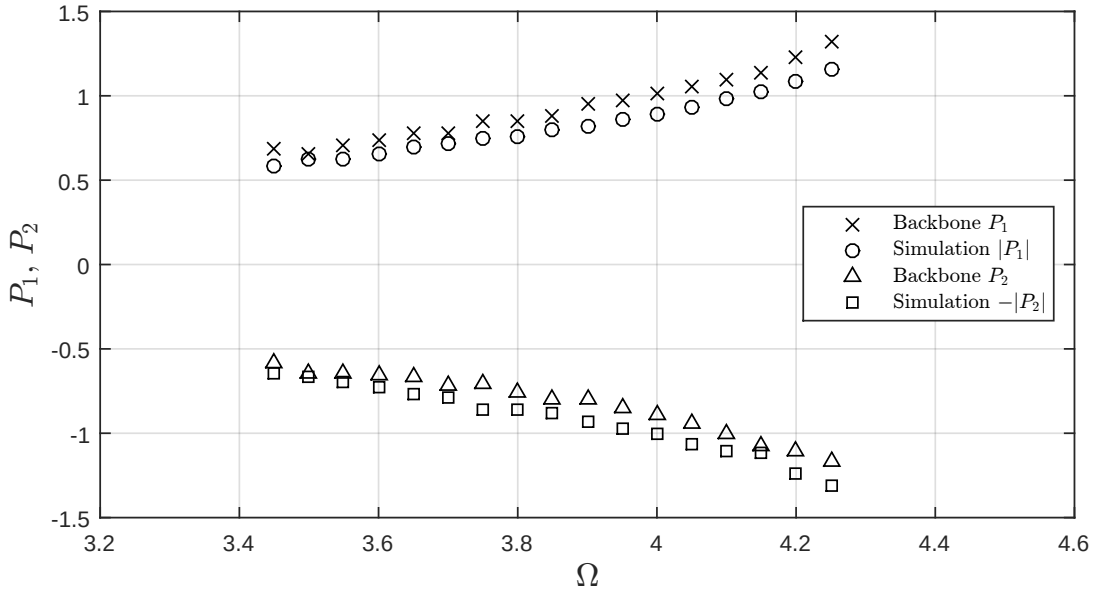

Figure 7: Comparison of simulation to forced and damped system for $\tilde{\mathbf{b}}_0/\Omega^2 = \{0.13, 0\}^T$

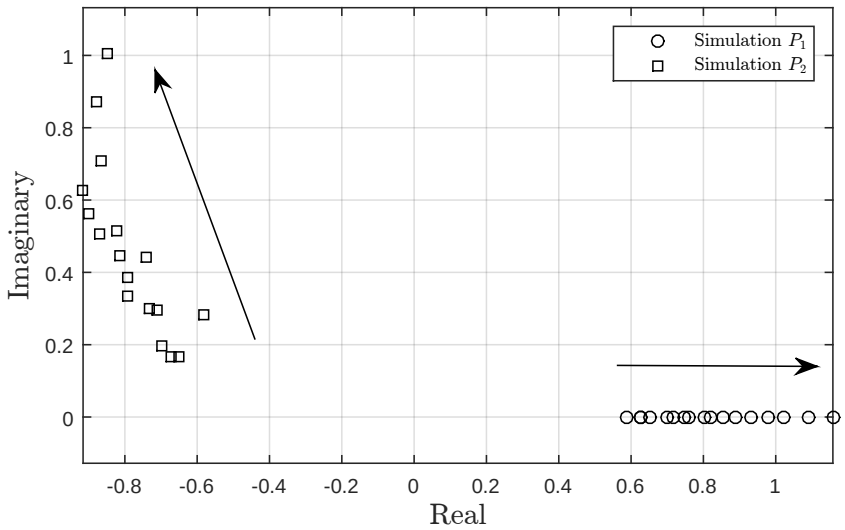

Figure 8: Complex amplitudes of the simulated response. Arrows indicate the general direction of increasing Ω for each set of points.

Much future work is required to further validate these findings and to further understand the stability and basins of attraction for these limit cycles, and how the underlying conservative system governs the response of the full rotor-stator contact system.

5 Acknowledgements

The research leading to these results has received funding from EPSRC grant number EP/G036772/1.

References

[1] G. Jacquet-Richardet, M. Torkhani, P. Cartraud, F. Thouverez, T. N. Baranger, M. Herran, C. Gibert, S. Baguet, P. Almeida, L. Peletan, *Rotor to stator contacts in turbomachines. review and application*, Mechanical Systems and Signal Processing, Vol. 40, No. 2, Elsevier(2013), pp. 401 – 420.

[2] J. Jansen, *Non-linear rotor dynamics as applied to oilwell drillstring vibrations*, Journal of Sound and Vibration, Vol. 147, No. 1, Elsevier (1991), pp. 115 – 135.

[3] S. Ahmad, *Rotor casing contact phenomenon in rotor dynamics – literature survey*, Journal of Vibration and Control, Vol. 16, No. 9, Sage (2010), pp. 1369–1377.

[4] A. Chiba, T. Fukao, O. Ichikawa, M. Oshima, M. Takemoto, D. G. Dorrell, *Magnetic bearings and bearingless drives*, Elsevier (2005).

[5] H. Bleuler, M. Cole, P. Keogh, R. Larsonneur, E. Maslen, Y. Okada, G. Schweitzer, A. Traxler, G. Schweitzer, E. H. Maslen, *et al.*, *Magnetic bearings: theory, design, and application to rotating machinery*, Springer Science & Business Media (2009).

[6] G. Schweitzer, *Safety and reliability aspects for active magnetic bearing applications-a survey*, Proceedings of the Institution of Mechanical Engineers, Part I: Journal of Systems and Control Engineering, Vol. 219, No. 6, IMechE (2005), pp. 383–392.

[7] F. F. Ehrich, *Observations of nonlinear phenomena in rotordynamics*, Journal of system design and dynamics, Vol. 2, No. 3, ASME (2008), pp. 641–651.

[8] F. F. Ehrich, *Sum and difference frequencies in vibration of high speed rotating machinery*, Journal of Engineering for Industry, Vol. 94, No. 1, ASME (1972), pp. 181–184.

[9] F. F. Ehrich, J. OConnor, *Stator whirl with rotors in bearing clearance*, Journal of Engineering for Industry, Vol. 89, No. 3, ASME (1967), pp. 381–389.

[10] R. Neilson, A. Barr, *Dynamics of a rigid rotor mounted on discontinuously non-linear elastic supports*, Proceedings of the Institution of Mechanical Engineers, Part C: Journal of Mechanical Engineering Science, Vol. 202, No. 5, IMechE (1988), pp. 369–376.

[11] W. Szczygielski, *Application of chaos theory to the contacting dynamics of high-speed rotors*, Rotating machinery dynamics, ASME (1987), pp. 319–326.

[12] F. F. Ehrich, *High order subharmonic response of high speed rotors in bearing clearance*, Journal of Vibration, Acoustics, Stress, and Reliability in Design, Vol. 110, No. 1, ASME (1988), pp. 9–16.

[13] A. Muszynska, P. Goldman, *Chaotic responses of unbalanced rotor/bearing/stator systems with looseness or rubs*, Chaos, Solitons & Fractals, Vol. 5, No. 9, Elsevier (1995), pp. 1683–1704.

[14] F. Chu, Z. Zhang, *Bifurcation and chaos in a rub-impact jeffcott rotor system*, Journal of Sound and Vibration, Vol. 210, No. 1, Elsevier (1998), pp. 1–18.

[15] S. Edwards, A. Lees, M. Friswell, *The influence of torsion on rotor/stator contact in rotating machinery*, Journal of Sound and Vibration, Vol. 225, No. 4, Elsevier (1999), pp. 767–778.

[16] E. V. Karpenko, M. Wiercigroch, E. E. Pavlovskaia, M. P. Cartmell, *Piecewise approximate analytical solutions for a jeffcott rotor with a snubber ring*, International Journal of Mechanical Sciences, Vol. 44, No. 3, Elsevier (2002), pp. 475–488.

[17] E. V. Karpenko, M. Wiercigroch, M. P. Cartmell, *Regular and chaotic dynamics of a discontinuously nonlinear rotor system*, Chaos, Solitons & Fractals, Vol. 13, No. 6, Elsevier (2002), pp. 1231–1242.

[18] E. Pavlovskaia, E. Karpenko, M. Wiercigroch, *Non-linear dynamic interactions of a jeffcott rotor with preloaded snubber ring*, Journal of Sound and Vibration, Vol. 276, No. 1, Elsevier (2004), pp. 361–379.

[19] E. Karpenko, M. Wiercigroch, E. Pavlovskaia, R. Neilson, *Experimental verification of jeffcott rotor model with preloaded snubber ring*, Journal of Sound and Vibration, Vol. 298, No. 4, Elsevier (2006), pp. 907–917.

[20] F. Chu, W. Lu, *Experimental observation of nonlinear vibrations in a rub-impact rotor system*, Journal of Sound and Vibration, Vol. 283, No. 3, Elsevier (2005), pp. 621–643.

[21] M. Torkhani, L. May, P. Voinis, *Light, medium and heavy partial rubs during speed transients of rotating machines: numerical simulation and experimental observation*, Mechanical Systems and Signal Processing, Vol. 29, Elsevier (2012), pp. 45–66.

[22] M. Cole, P. Keogh, *Asynchronous periodic contact modes for rotor vibration within an annular clearance*, Proceedings of the Institution of Mechanical Engineers, Part C: Journal of Mechanical Engineering Science, Vol. 217, No. 10, IMechE (2003), pp. 1101–1115.

[23] P. Keogh, M. Cole, *Rotor vibration with auxiliary bearing contact in magnetic bearing systems part 1: Synchronous dynamics*, Proceedings of the Institution of Mechanical Engineers, Part C: Journal of Mechanical Engineering Science, Vol. 217, No. 4, IMechE (2003), pp. 377–392.

[24] K. Mora, C. Budd, P. Glendinning, P. Keogh, *Non-smooth Hopf-type bifurcations arising from impact-friction contact events in rotating machinery*, Proceedings of the Royal Society A, Vol. 470, The Royal Society (2014), pp. 3353–3375.

[25] Y.-B. Kim, S. Noah, *Quasi-periodic response and stability analysis for a non-linear jeffcott rotor*, Journal of Sound and Vibration, Vol. 190, No. 2, Sage (1996), pp. 239–253.

[26] G. Von Groll, D. J. Ewins, *The harmonic balance method with arc-length continuation in rotor/stator contact problems*, Journal of sound and vibration, Vol. 241, No. 2, Sage (2001), pp. 223–233.

[27] A. Zilli, R. J. Williams, D. J. Ewins, *Nonlinear dynamics of a simplified model of an overhung rotor subjected to intermittent annular rubs*, Journal of Engineering for Gas Turbines and Power, Vol. 137, No. 6, ASME(2015), p. 065001.

[28] A. D. Shaw, D. A. W. Barton, A. R. Champneys, M. I. Friswell, *Dynamics of an mdof rotor stator contact system*, in *Proceedings of the 34th IMAC, A Conference on Structural Dynamics*, SEM (2016).

[29] A. Shaw, A. Champneys, M. Friswell, *Asynchronous partial contact motion due to internal resonance in multiple degree-of-freedom rotordynamics*, Submitted.

[30] M. I. Friswell, J. E. T. Penny, S. D. Garvey, A. W. Lees, *Dynamics of Rotating Machines*, Cambridge (2010).

[31] K. Worden, G. R. Tomlinson, *Nonlinearity in Structural Dynamics*, Bristol: Institute of Physics (2001).

[32] D. J. Wagg, S. A. Neild, *Nonlinear Vibration with Control*, Dordrecht: Springer (2009).

[33] T. L. Hill, A. Cammarano, S. A. Neild, D. J. Wagg, *Interpreting the forced responses of a two-degree-of-freedom nonlinear oscillator using backbone curves*, Journal of Sound and Vibration, Vol. 349, Elsevier (2015), pp. 276–288.

[34] A. Cammarano, T. L. Hill, S. A. Neild, D. J. Wagg, *Bifurcations of backbone curves for systems of coupled nonlinear two mass oscillator*, Nonlinear Dynamics, Vol. 77, No. 1-2, Elsevier (2014), pp. 311–320.